Received: 16 December 2023 | Accepted: 27 March 2025

DOI: 10.1002/nsg.70004

Near Surface Geophysics EAGE EUROPEAN ASSOCIATION OF GEOSCIENTISTS & ENGINEERS

ORIGINAL ARTICLE

Electromagnetic survey of old landfill boundaries—A case study

Pauli Saksa[1] | **Milja Vepsäläinen**[2]

[1]Geosto Oy, Helsinki, Finland

[2]EnviPro Oy, Helsinki, Finland

Correspondence
Pauli Saksa, Geosto Oy, Helsinki, Finland.
Email: pauli.saksa@geosto.fi

Abstract

This case study examines the mapping of old landfill boundaries using a short-coil spacing frequency domain electromagnetic (EM) system in western Finland. Geophysics was used to supplement the preceding soil drillings, test pits and samples taken. In many places at the site area, there were difficult access conditions and obstacles that flexible moving geophysical surveying could bypass and avoid. Short-coil spacing EM mapping with three frequencies was chosen as the method of investigation. The frequency-sounding effect was analysed and shown that it is present under typical conditions met. The depth of investigation can also be calculated with the specific system parameters specified. Frequency-traverse tabulated graphical presentation of apparent resistivities was aefficient method to present EM results for qualitative assessment. In practice, on-site applicability was first tested with two reference lines for natural ground and landfill area characteristics. The results showed clear differences in terms of resistivities, as well as the real (Re) and imaginary (Im) component values, Re/Im ratios and signal characteristics. The main survey consisted of another 20 investigation lines at various places intersecting presumed landfill boundaries. Interpretation of the data and point-by-point classification were based on reference line data and inferred waste disposal material indicators. The quality of the data was assessed with calibration points and static offsets determined with the help of resistive bedrock point. Finally, EM data values were compared against test pits and drillings at close proximity, supporting the reliability of the EM survey and the differentiation between waste and contamination made. Layer modelling was tested to study the depth penetration and to assess whether additional information could be produced from calculated resistivities and magnetic material indications.

KEYWORDS
case histories, electromagnetic, environmental, interpretation

INTRODUCTION

This case study discusses the mapping of old landfill boundaries using a short-coil spacing electromagnetic (EM) system. The landfill area is located in the suburb of Suvilahti in Vaasa, in western Finland. The municipal and industrial waste landfill site was used in the 1960s until a nearby waste disposal area was taken into use. The study area is 7 ha in size, spanning 100–200 m from E to W and 500 m from N to S. After disposal, the site was covered with a thin layer of soil and inhabited by small industrial facilities which were distributed over the allocated area. A prior investigation carried out in 2009 estimated that the waste volume in the area would be around 65,000 m^3.

The City of Vaasa is considering a new city plan for the area and therefore requires more exact information regarding soil contamination and landfill area boundaries. Site investigations and results also enable risk assessment. There were also five non-built industrial real estate properties in the area which could not be developed without a risk assessment procedure.

Geophysical surveying was considered to assist further in mapping the landfill boundaries, particularly in places with no machinery access, where data were sparse or missing, or where results from test pits were not clear. There was a need for more data indicating waste occupancy so that the representativeness of physical samples could be confirmed. Waste deposition varied from continuous volumes to scattered spots. Geophysics was also considered a rapid method for mapping continuous line data and flexibly covering the site. Geophysical measurement can also record information from a larger volume than direct sampling.

At the pre-survey stage, there were significant uncertainties surrounding site conditions. It was not known if and how lines could be established without influences from surface objects, how various places of interest could be accessed, or whether suitable and continuous profiles for measurements could be run inside industrial properties. Google's Street View map service covered most of the roads in the area, providing useful views for pre-survey planning.

We present this survey and research as an example of how geophysical EM mapping can be utilized as an efficient and rapid method to supplement landfill area screening in demanding site conditions. It also depicts that applicable survey configuration and interpretation require a site-specific bespoke procedure.

SITE DESCRIPTION

Site conditions and geology

A site investigation report (Vahanen Environment Oy, 2015) summarized the legacy data and data from the 2014 investigations before the geophysical survey. The approximate boundaries of the landfill site were estimated using screening results from 2009 to 2014 studies. Investigation points were selected at accessible locations to cover the unknown landfill area. The primary investigation method was 26 test pits and 5 soil drillings, combined with soil sampling and laboratory analyses. In addition, test pits and percussion drilled samples were studied to map soil types and waste materials. Soil descriptions and sampling were carried out at 0.5 m intervals down to a depth of 2–3 m in order to reach the natural soil. Surface and groundwater samples were taken from two and three points, respectively. Penetrative investigation locations were controlled by access restrictions and avoidance of existing underground infrastructure. A report (Vahanen Environment Oy, 2015) proposed that a risk assessment be carried out for the area based on results from 2014 investigations.

Figure 1 shows the site, including the locations of test pits, boreholes and soil contamination levels together with waste observations. The red line outlines the estimated landfill area. Squares depict test pits, and circles indicate percussion drillings and groundwater monitoring wells. The colour coding of the square symbols indicates waste observations: black for waste, while empty for no waste. Soil contamination level is indicated with blue for hazardous waste, red for exceeding the upper guideline values, orange for exceeding the lower guideline values and grey for levels surpassing the threshold values. This classification is based on the Finnish Government Decree 214/2007 concerning the assessment of contaminated land and the necessity for remediation. In industrial areas, points marked in red and blue exceed acceptable concentrations of soil contaminants. The estimated landfill border is based on points between non-contaminated and contaminated sampling locations, waste observations, legacy air photo and map data and topographical indications, such as observable ground fills. Geological site description was non-existing.

Some parts of the area were barren as a result of daily industrial or storage activities, but frequently contained scrap, property fences, obstacles and abandoned metal structures. In addition, the site was characterized by ground fills and large boulders, small ponds, wet pits and dense forests or bush. Accessing the experimental points was not a straightforward process. Penetrative investigations were limited by the aforementioned factors, and underground cables and channels also prevented activities.

Other urban objects in the area include a 20 kV power line crossing the site, a biogas pipeline, a pumping station on the eastern border and power lines along main roads bordering the site, marked in Figure 3 later in the text.

The Baltic Sea is approximately 2 km to the south of the site. The topography is very flat; mostly less than 3 m above sea level. Only a few spots have elevations higher than +4…+5 m, and inside the survey area the lowest elevations are approximately +1.0 m. Groundwater is found at a shallow depth of 1.5–2.0 m below the soil surface, and after rain, it is sometimes only 0.5 m below the surface. In some test pits, groundwater was not detected, indicating heterogeneity in hydraulic conductivity. A small ditch runs through the area from NNE to SSW towards the sea, and some ponding has taken place along it.

The natural soil beneath the fill consists of clay or muddy clay. In the north-western corner, a small subarea with a surface layer of sandy moraine has been identified.

The bedrock type is metamorphic biotite paragneiss originating from the Archean Svecofennian era. There are no direct drilling results of the bedrock depth, but nearby weight soundings observed a soil thickness of a few metres. The Geological Survey of Finland's soil and bedrock map service 'Maankamara' gives rough estimates of 10 m and 30 m for total soil thickness for the northern and the southern parts of the study area, respectively.

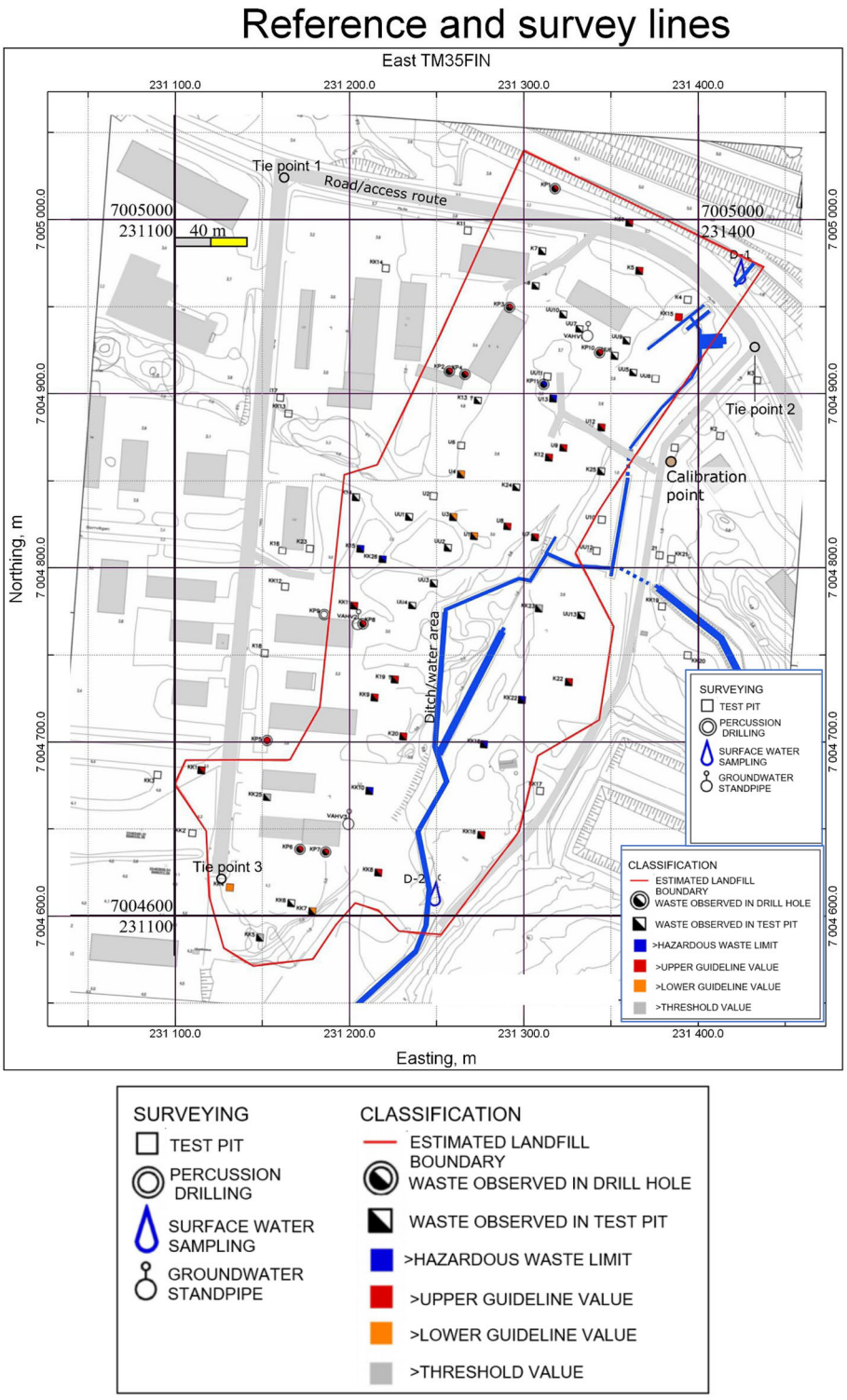

FIGURE 1 Site map with the results of the prior investigation (2009–2014) and landfill borders. Blue lines indicate ditches and ponding.

The waste is covered by surficial soil consisting of sand, gravel, moraine and crushed material, with a thickness varying between 0.5 and 2.0 m. In some non-built areas, the surface layer is very thin or non-existent. Yard areas are paved with asphalt.

Waste materials and water

Below the topsoil, the landfill comprises a mixture of waste and soil, averaging 1.0 m in thickness. The waste materials in the landfill are diverse, primarily consist-

ing of municipal and organic waste, as well as plastics, glass, concrete, wood and metals. Industrial waste consists of metal hydroxides and zinc waste, PAH compounds and petroleum hydrocarbons. In soil samples, Hg, Cd, Cu, Ni, Zn and Pb exceeded the upper guideline values, along with hydrocarbons and PCB compounds. Cu and Zn values in particular frequently exceeded the upper guideline values.

At the Suvilahti site, the waste material, the leachate and the groundwater have high electrical conductivity (EC), so the target would likely differ from natural clay conductivity, although this was not certain. Ground fills like sand, moraine or gravel without waste have low EC. Therefore, areas filled with non-waste materials would differ from natural clay or fill containing waste. It was also considered that as waste landfills are heterogeneous with strongly varying conductivity, they would differ from homogeneous natural clay or moraine coverage, which display low variability in conductivity.

Surface water collected from the ditches was analysed for harmful substances. The concentrations were only slightly elevated compared to natural water. All the groundwater samples had high concentrations of hydrocarbons, metals and other analysed contaminants. The EC and oxygen consumption of the water samples corresponded to typical municipal waste landfill results. ECs of the water samples ranged from 50 to 300 mS/m (resistivity 3–20 Ωm, $T = 25°C$). In a nearby groundwater station, the water's EC was 51 mS/m (19.6 Ωm). Fresh groundwater has an average value of 6.4 mS/m (154 Ωm) in Finland, and limit values for a range of 10%–90% are 2.4–11.8 mS/m (410–85 Ωm) (Soveri et al., 2001).

METHODOLOGY

Literature review

Suitable surveying methods for the site conditions were ground penetrating radar (GPR) or magnetic or EC measurements. However, GPR was rejected due to the minimal penetration in clay. Both magnetic and EC measurements would be suitable for mapping metallic waste. There are two categories of EM instruments: Those that are directly calibrated to display EC values and those that record the real (Re) and imaginary (Im) components of the EM field, which are subsequently processed into units of interest, such as EC. The real component is also called the in-phase and imaginary is known as the quadrature or out-of-phase component. The terminology used varies in literature.

EC-based measurements have long been utilized in the characterization of landfills. The textbook by Reynolds (2011) describes how EC measurements (electrical and EM) have been used extensively and successfully employed to map the characteristics of waste deposits and to delineate potential leachate migration, usually over closed landfills. Reynolds emphasizes that there is no such thing as a typical landfill; there are many physical variables. Care must be taken not to presume a particular geophysical response for any given location. In his 2011 publication, Reynolds (2011) has compiled a list of potential unknowns for any landfill, including the type of void space, type of lining, type of capping, site dimensions, tipping history, geological factors and characteristics related to infill material.

Godio and Naldi (2009) applied DC and EM methods to a small 200 × 50 m area to map 2–3 m thick surface part compounded by man-made debris from automotive demolition and other types of waste. EM surveying used Re- and Im-components in data analysis to differentiate between ferrous material and leakage effects. Mitsuhata et al. (2014) studied a Japanese site contaminated with VOC and hydrocarbons and observed that EM induction mapping enabled efficient coverage of the study area and imaging up to a depth of 10 m. Surveying was found to be a useful technique to delineate the infiltration pathways of contaminants. Direct push in situ measurements were used to verify the interpreted resistivity structure as there were several conductive layers present, including clay.

Deldago-Rodriguez (2017) used EM profiling to detect hydrocarbons and scrap metals at a 48 ha industrial waste dump site. The survey detected low resistivity anomalies related to mature pollution which further guided the positioning of the drilling points. Metals were detected by EM in-phase anomalous values (instrument measured in-phase values in ppt, parts per thousand). The site allowed for the systematic use of continuous perpendicular profiles.

Narciso et al. (2020) presented a geostatistical EM inversion for landfill characterization. They used both Re- and Im-component data to solve EC and magnetic susceptibility.

Dumont et al. (2017) concluded that frequency domain EM methods are powerful in characterizing landfill deposits due to their simultaneous sensitivity to EC and magnetic susceptibility. However, resolving details can be challenging because of the complex composition of waste deposits and the heterogeneous distribution of material components.

A large research group led by Inauen et al. (2019) studied several methods for landfill characterization in the United Kingdom. They observed that EM and magnetics were able to provide a rapid overview of landfill structure and detected areas with higher metal content. Additionally, rapid EM methods can also be used to plan profiles for more time-consuming methods like induced polarization and electrical resistivity tomography.

Quite recently, Mitsuhata et al. (2022) studied a drone-borne EM survey system for searching for metallic objects and the mapping of resistivity. The

Re-component was used to identify metallic objects (buried vehicles), whereas the Im-component was employed to characterize wet and dry soil fields.

Electromagnetic mapping and instrument

EC mapping using an EM induction-based system was selected for this study. The method detects both conductivity and magnetic infillings. The estimated contrast between natural clay soil and soil fills could also indirectly outline the landfill area.

From an EC point of view, it was possible to classify the types of basic materials. Clay in the area has a resistivity of 10–40 Ωm. Sandy moraine has a higher resistivity than clay, starting from 100 Ωm. Soil fills (gravel, sand and other fills) have a higher resistivity than sandy moraine, above a level of 100 Ωm. Metals have very low resistivity, and waste that contains iron can also have high magnetic susceptibility. Soil materials located above the groundwater level are in a non-saturated state, and their resistivities can be two or more times higher than those of similar saturated soils. In Finland, crystalline metamorphosed bedrock typically has very low porosity (<1%) and resistivity is high, over 1000 Ωm. When present, fractured and crushed zones can yield lower resistivity values.

An EM profiling (EMP)-400 Profiler from Geophysical Surveying Systems Inc. was used for EMP and mapping. This system features a compact and short 1.22 m transmitter-receiver (Tr-Rc) dipole–dipole configuration, which can operate in HCP or VCP geometry modes. HCP denotes horizontal coil profiling (vertical dipoles), and VCP denotes vertical coil profiling (horizontal dipoles). The surveying height is selectable, either at hip height or at a lower level using the carry handles. Frequencies can be selected between 1 and 16 kHz, and frequencies of 4, 12 and 16 kHz (4000, 12,000 and 16,000 Hz, respectively) were selected. Two high frequencies were chosen for very near-surface coverage and to provide high signal levels, whereas the lower frequency of 4 kHz is to cover deeper surface layers. Frequencies in the very low range of 1–2 kHz typically exhibit low response levels and are susceptible to a low signal-to-noise (S/N) ratio.

Two additional factors facilitated the use of EM system. It is handy to operate in difficult terrain, and no cables or direct contact with the ground are required. Additionally, the footprint of several metres around each measurement point meets the larger volume sampling and averaging criteria mentioned in the 'Introduction' section.

The recorded values are real (Re) and imaginary (Im) component magnitudes in parts per million (ppm) at each frequency. Re-component values, however, are not absolute, a topic that will be discussed later in the 'Results' section. The depth penetration of at least a few metres at all frequencies was adequate, as the waste materials were situated close to the ground surface.

Depth of investigation and frequency effect

Depth of investigation (DOI) and frequency effects with small spacing dipole–dipole systems have long been a topic of discussion. Reynolds (2011) also mentions a long-running disagreement between manufacturers over the validity of an instrument with a fixed-coil separation providing real-depth discrimination by changing the frequency. An important parameter in this context is the induction number B, which is defined as follows:

$$B = \sqrt{(\sigma\mu\omega/2)} \bullet r,$$

where σ is EC (S/m), μ is absolute magnetic permeability (Wb/Am), ω is angular frequency $2\pi f$, where f is frequency in Hz (1/s), and r is the mutual distance between transmitter and receiver coils (m).

A major misleading concept has been the use of the conductance type of multi-layer responses and summation introduced by McNeill (1980) within the low induction number (LIN) range. This concept is widely disseminated and has been extensively utilized by users of conductivity meter instruments. However, this approach overlooks the influence of frequency, relying on a theoretical framework that appears valid. It establishes a coil geometry-based rule for the DOI and for calculating the layer model response. One of the cornerstones of this approach is that frequency (over LIN range) has no effect. It is stated that the DOI is a maximum of approximately one to two times the coil spacing.

Already, decades ago, Spies and Frischknecht (1991, pp. 308–309) listed conditions under which the aforementioned LIN range approach is valid for small-coil spacing systems and layered earth response analysis. Several conditions must be met, the most critical being that the induction number B must be less than 0.02 in all considered layers. This condition is rarely satisfied, and therefore, the DOI consideration based on the geometric conductance model, without accounting for frequency effects, is not applicable in most encountered situations.

In his article on small induction sensors, Won (2003) states that the following characteristics must be met in order for depth sounding to be possible. The system must possess sufficient sensitivity to resolve the small frequency dependence in a resistive area, a large dynamic range to accommodate near-surface conductivity effects, and the ability to avoid certain frequencies with high noise levels—such as those caused by power lines. An instrument with ppm recording accuracy and which covers a sufficient frequency range has frequency-sounding capability, although limited. Huang

(2005) examined depth penetration and concluded that it is approximately the square root of the calculated skin depth. The term is used in the context of the far EM field (far from the source, also called wave zone) and in plane wave theory. It determines when the field component amplitudes have attenuated by a factor e. The skin depth is defined by the formula $\delta = \sqrt{(2/\sigma\mu\omega)}$, and under normal free-space conditions, the alternative formula $\delta = 503.2\sqrt{(\rho/f)}$ can be applied, where ρ represents resistivity (Ωm) (e.g., Reynolds, 2011). In the context of small coil spacing systems and the near-field range, skin depth serves as a practical measure that does not have a direct relationship to the physics from which it originates.

Andrade et al. (2016) studied the differences between values obtained using the LIN approximation and those derived from the exact numerical modelling for small coil spacing conductivity meters. They concluded that the apparent conductivities calculated with the LIN approximation diverge from the ideal curve(s) even at LINs (less than 0.05). Furthermore, they asserted that the LIN approximation equation should not be used, nor should any other linear calibration.

Saksa (2016) presented precise numerical modelling results for a variety of two-layer models for HCP and VCP coil systems across a frequency range of 0.5–32 kHz and with coil heights of 0.1 and 1.0 m. It concluded that approximate layer modelling frequently fails when a more conductive ground is situated below a resistive surface layer. The differences were greatest at the high-frequency end used. Differences increased with coil height and were larger for the VCP configuration. The square root of the skin depth yields a good approximate value for maximum depth penetration in HCP geometry. With multi-frequency hand-held systems, depth penetration is typically much larger than the coil spacing used. Therefore, employing precise numerical modelling is preferable, as the validity of the approximate solution can vary considerably within an area surveyed in the field.

We can clarify the DOI and frequency effect using the concrete example presented below. Responses are calculated for an EMP-400 Profiler instrument, operating in both HCP and VCP modes, with coil spacing of 1.22 m, coil height of 0.2 m and frequencies ranging from 700 Hz to 40,000 Hz. The model is a three-layer earth, with the top two layers having thicknesses of 3.0 m. The resistivities from top to bottom are 500, 50 and 5 Ωm, which makes them typical, including in the light of our Suvilahti recorded resistivities, which are shown later.

Figure 2a illustrates the HCP responses for Im and Re-components. The highest Im and Re values in ppms are recorded for three-layer model, the second-highest for the case where two bottom layers are set to an intermediate layer value of 50 Ωm (layer interface at 3.0 m), and the lowest values (Im) for a homogeneous 500 Ωm half-space situation as a reference. The example unequivocally depicts that each layer has a distinct and measurable influence on EM responses. The first layer interface, situated at a depth of 3 m, corresponds to 2.45 times the coil spacing, and the second interface at 6 m is 4.9 times the coil spacing. The Re components exhibit similar behaviour, although their response amplitudes are smaller.

The frequency effect is evident, demonstrating the capability for frequency sounding. If there is no frequency effect, responses vary by frequency; the response at 4 kHz is 10 times less than that at 40 kHz. However, in the case of the three-layer HCP, the response at 4 kHz is 2.24 times greater than what the frequency ratio would predict, and at 1 kHz, it is 2.91 times greater.

Figure 2b displays the modelling results for VCP configuration, not utilized in the Suvilahti case. As they have three layers with increasing conductivity, the model responses differ from those of the two-layer model. The response amplitudes are smaller, which is a known characteristic feature. The depth penetration is also less in VCP mode, as evidenced by the diminished influence of the third bottom layer. In the HCP model, the bottom layer at 10 kHz increases response amplitudes from 127 to 294 ppm, and in the VCP model, the increase is less, from 79 to 162 ppm.

In light of the data and the referenced examples, it is clear that the LIN range geometric conductance model should not be used or referenced for DOI estimation and in EC data inversion. The conductance model can be applied to make the height correction for the system over a homogeneous half-space; all other uses are subject to significant errors, varying case by case. It is also important to note that using the LIN range formula in the conversion of Im-component values to apparent resistivities does not imply that the LIN range geometric conductance model (McNeill, 1980) is valid and applicable. It is just a linear relationship that holds over a limited range of induction numbers. Furthermore, when using conductivity meters and the LIN approximation, it is not straightforward to understand or apply the relationship between the induction number and EC.

It is important to address one additional issue in this context and discussion. The aforementioned maximum penetration depth does not imply that all layers and other forms of volumes are detected within this depth range. EM systems are sensitive to electrically more conductive layers and insensitive to embedded layers or objects that are more resistive. Only the first surface layer makes an exception. In order to be recognizable, layers must also have large enough conductance (thickness x conductivity) within the depth that the EM wave penetrates. The same applies to 2D objects and 3D volumes. In general, within the maximum penetrated depth range, conductivity contrasts in the lower half must be large enough

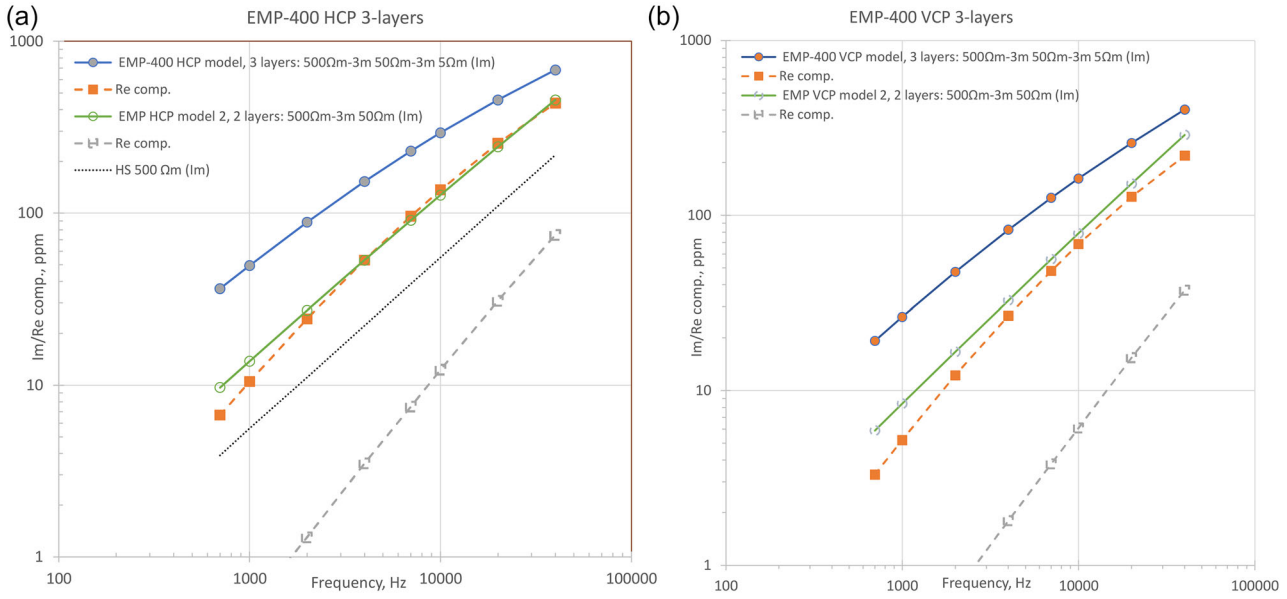

FIGURE 2 Horizontal coil profiling (HCP) and vertical coil profiling (VCP) responses of a two- and three-layer earth for an EMP-400 type of frequency domain small-coil spacing instrument.

to be detectable, and target volumes must be considerably larger than those near the surface. In addition, for an anomaly to be detected, the presence of noise in the data and subsurface homogeneity play important roles. In practice, it is good to analyse DOI for a typical target of interest before proceeding with data analysis.

The EMP-400 Profiler is factory pre-calibrated for zero response and features a three-phase site calibration procedure for selected surveying parameters. The first response is measured with the instrument placed alone on the ground surface in configuration selected, the second phase involves the user and PDA at the measurement height, and the third phase records the remaining real (Re) component level for later subtraction. The calibration was conducted on site after the site inspection and when surveying height was decided. The standard procedure is to carry out a site calibration at Geosto's test site under known conditions and established lines, supported by multiple time-lapse datasets to identify any deviations.

Figure 3 illustrates the conditions at the Suvilahti site, featuring a soil map, the estimated landfill boundary line marked in red, ditch/water areas and power and biogas lines. The observational design areas identified for measurement profiles are indicated by ellipses. Three red ellipses denote locations where waste fill is present at all points; these areas were considered to be reference points containing waste. Areas marked with green ellipses were considered probable no-fill reference points. Brown ellipses indicate about 20 places where it was considered possible to run experimental measurement profiles and also where the landfill boundaries were uncertain or where drillings and test pits were missing.

One geological cross-section is presented in Figure 4, with its location indicated in Figure 3 by a line labelled A–A′. This section demonstrates that there was very limited information of subsurface conditions and geology. Sand or soil fill and waste were documented within the site, with the clay layer either removed or located at the bottom. Points UU1 and UU indicate that similar sand and clay can be found both inside and outside the landfill area.

Data collection and presentation

The on-site objective was to measure as many data samples as possible along short, continuous profiles over the outlined landfill boundaries. In other words, to delineate the landfill boundaries in more detail and to study how waste is distributed and how distinct the waste area boundaries are.

Moving among industrial facilities, their fences and storage areas (metal structures, scrap, huts, machinery, etc.) was demanding and required on-site planning and decisions. Survey lines could not be marked in advance, and obtaining continuous profile recordings required free-form lines to avoid disrupting existing infrastructure.

Measurements took place over 2 consecutive days in the spring of 2015. Initially, the prevailing conditions were assessed. The vegetation was predominantly low, dry and sparse, which led to the selection of the low carrying mode. Measuring close to the ground (h = 0.2 m)

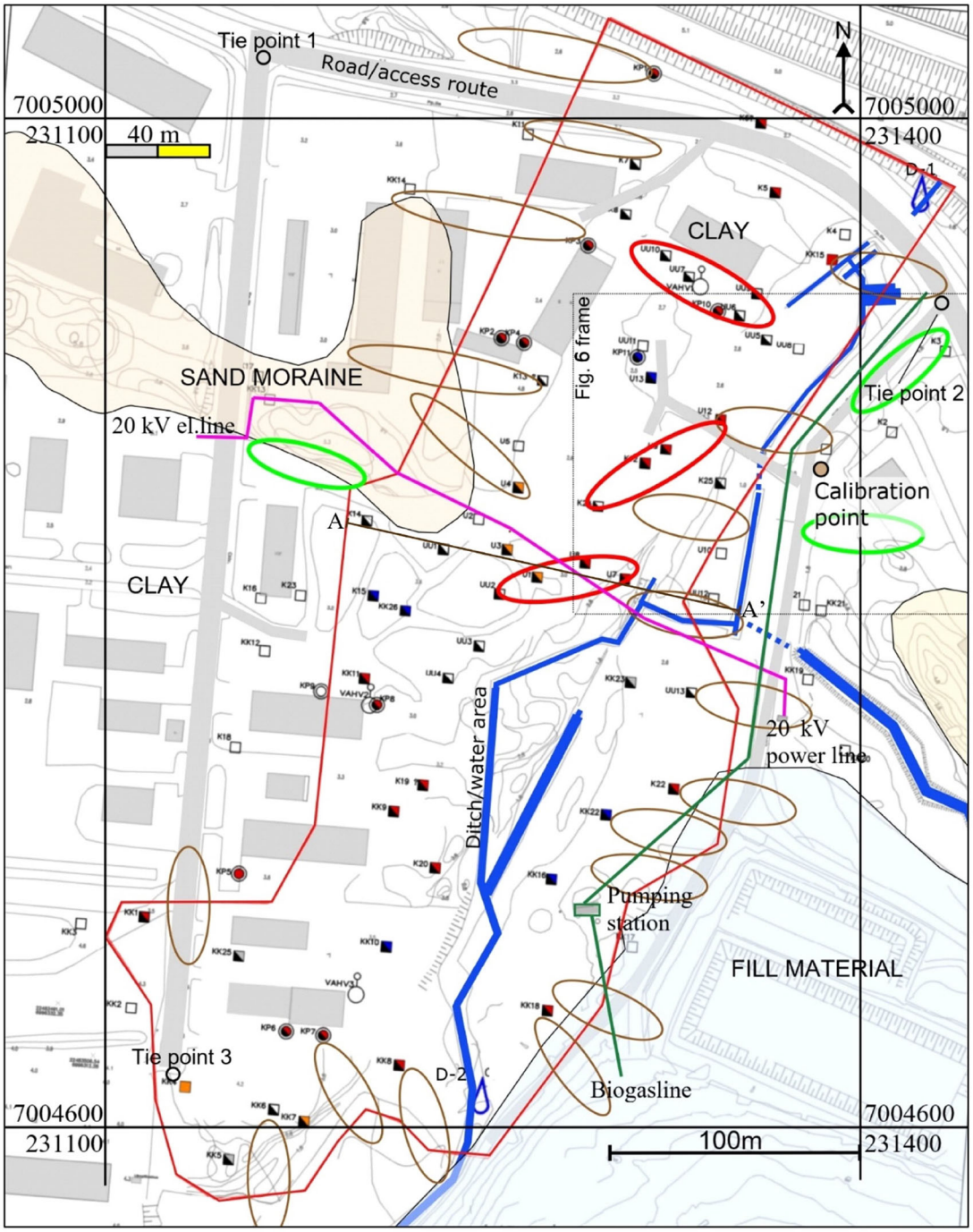

FIGURE 3 Site map with planned surveying places, soil types and subarea objectives.

doubles the signal level compared to recordings taken at hip height (h = 1.0 m). The calibration point (shown in Figure 2) was chosen from the roadside along the eastern access, where the EMP-400 Profiler was site- and user-calibrated. The EMP-400 has three measuring modes: stationary, continuous and free-form. In the stationary mode, each recording is triggered by the user, whereas continuous mode captures data samples by stacking over a predetermined time interval. In continuous mode, there is also a free-form surveying mode available using GPS and simultaneous data display as a map on the PDA screen. In Suvilahti, continuous mode with a 4-s recording interval was employed, resulting in a stack of 16 recordings (each recording takes 0.25 s when using 3 frequencies). Therefore, in continuous mode, the point separation calculated from GPS data indicates the propagation speed at 4-s intervals. For some shorter lines, stationary mode was used to bypass some

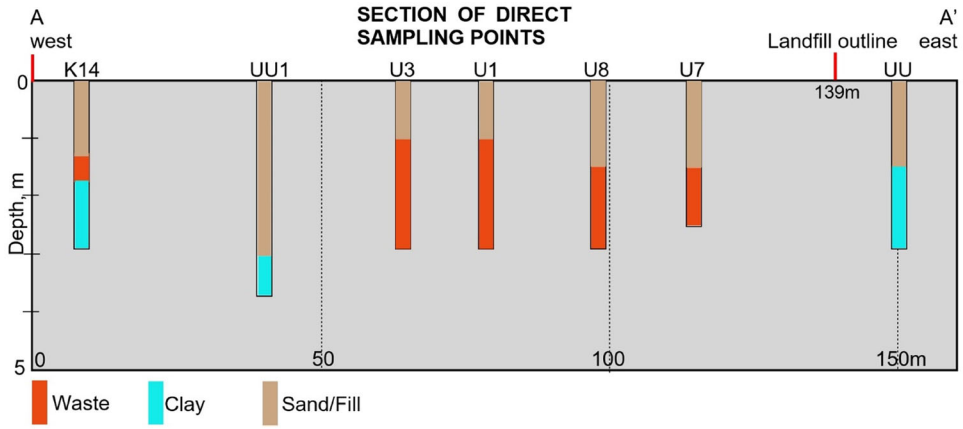

FIGURE 4 Cross-section A–A′ depicting direct sampling data.

obstacles or objects. This approach allows for the selection of the measurement location and yields the highest quality recordings obtainable. Data smoothing was disabled during recording.

The measured lines were free-form, so GPS positioning-based recording was enabled. The PDA uses a WAAS (Wide Area Augmentation System) GPS recording mode and WGS84 output as GGA text strings. The values were converted to ETRS-TM35FIN *X* and *Y* coordinates. Three tie points displayed in Figure 1 were measured for TM35FIN adjustment and to compare WGS84 coordinates with exact *X* and *Y* values. We present the line traverse in profiles as stations, as the distance becomes overestimated due to small scattering in the *X* and *Y* values, which cumulate.

Two pilot lines, L1 and L2, were measured: Line L1 for natural ground characteristics in the area south of tie Point 2 (Figure 3; green ellipse) with 23 points. Line L2 was positioned in the known landfill area (Figure 3; middle red ellipse area) and comprised 41 points. In L2 measurements, a few metres' distance was maintained from all disruptive surface objects. The average propagation speed along these two lines was 0.4–0.5 m/s.

Apparent resistivities can be derived through a linear transformation of Im-component values within the LIN range, taking into account the measurement height. Conversion follows the response curve and is valid with high accuracy up to an induction number *B* value of ~0.8. At that point, Im-component values attain magnitudes between 80 and 90,000 parts per million (ppm). When $B < 0.8$, Re-component magnitudes are consistently lower, or much lower than Im-values, and with $B \geq 1.0$, they are higher than Im-component values. At very high *B* values (>10), the Re-component saturates at −1,000,000 ppm (=−100%) and the Im-component approaches a value of −0 ppm. Re- and Im-component behaviour for various loop configurations, along with the corresponding phasor diagrams, are discussed and presented, for example, by Frischknecht et al. (1991).

However, in the case of 2D and 3D electrical conductors, the values of the field component values do not need to be that high when Re-component can be larger than the imaginary one. For example, when the object has some distance from the loop system. So, Re/Im ratio of >1 is a fairly good indicator of metallic type waste and is generally considered an indicator of a good electrical conductor in EM exploration.

In resistivity mapping, soundings data are frequently presented as pseudosections for qualitative assessment and interpretation. An apparent resistivity pseudosection requires that the apparent depths form a coherent geometric pattern. Because of square root of skin depth relationship and the frequencies used in Suvilahti case, this does not happen. For an earth resistivity of 100 Ωm, depth penetration at 4 kHz is 8.9 m as maximum and 6.8 m and 6.3 m for 12 kHz and 16 kHz, respectively. This setting does not favour interpolation. Frequency 12 kHz does not significantly differ from 16 kHz, and as resistivity is decreasing with depth, the differences become even smaller. An example pseudosection, represented as colour bars, is provided for Line L1 in Figure 4, located below the tabulated frequency-traverse apparent resistivity section.

Negative Re- and Im-component values are also frequently present and originating from 2D and 3D objects and in resistive low amplitude ends caused by noise in data. This leads to negative non-physical apparent resistivities in LIN range conversion. Negative value does not allow calculation of apparent resistivity and approximate depth penetration. Estimation of depth penetration requires also that homogeneous or layered earth is valid, but negative values indicate that this setting is not present.

The calculation of pseudosections becomes awkward when negative apparent resistivities are among the ones interpolated. But negative values, both in Im- and Re

components, are important in general ground and object type classification and in discrimination. In tabulated frequency-traverse graphics, negative apparent resistivities show up in very low resistivity end, and colouring is used which is, in fact, indicative; they arise from electrically conductive 2D or 3D objects, so objects belong to waste mass.

That is why it was advantageous to present the converted apparent resistivities in a frequency-traverse tabulated format. Each cell value can be examined, along with the mutual cohesion of the data.

Line L1 results are presented as an apparent resistivity (ρa, Rhoa) frequency-traverse graphical listing, along with the Re-component profile, as shown in the upper section of Figure 5. For comparison, the middle section displays the apparent resistivity depth (pseudo-)section according to penetration depths calculated for each frequency. Line L2 results are given in the lowermost part of Figure 5, with the highest frequency positioned at the top of the presentation. Exact point locations are displayed in Figure 6, where the line code indicates the starting point of the line, and the arrow denotes the direction of propagation.

The natural soil reference Line L1, which has a length of 38 m and station spacing of 1.7 m, is not completely situated in natural, undisturbed conditions. Apparent resistivities vary greatly at stations 5–7 and 13–14, with Points 13–14 also recording substantial negative Re-component values. Apparent resistivities lie between 20 and 50 Ωm at all other points and at all frequencies. About 75% of the recorded line length reflects characteristics of the natural area; however, the two local exceptions mentioned do exist.

Line L2 was placed in an area where most test pits and drilling points contained waste. The line has 41 measurement stations with an average spacing of 2.0 m (length 80 m). The apparent resistivity profile is smooth except at Points 7–8 and 19–23, which have rapid variations. Very low resistivities of 1–5 Ωm were detected at stations 7–8. Notably, in the first part of the profile, the resistivity level is very low, between 2 and 10 Ωm, but rises to a range of 10–25 Ωm after an anomalous middle section. The Re-component has continuous, strong anomalies, except for the first four points at the beginning of the line. The anomalies give positive readings, except at Points 19–21, which have strong negative anomalies and side maximums both in Im- and Re-components, indicating a narrow subsurface electrical conductor below stations 20–21.

Data at all three frequencies correlate strongly as expected, which increases reliability. About 85%–90% of the 80-m-long profile clearly indicated a signal from disturbed ground and oscillating characteristics originating from waste material. It is to be noted that the EMP-400 Profiler's Re-component readings are not absolute (in ppm). In general, they are too large when compared to the Im-component values but do function reliably as qualitative indicator values. Re/Im ratio $\gg 1$ indicates well presence of metallic objects.

Although the above-mentioned analysis could not be carried out completely on site, component levels, variability and characteristics were noted immediately during start-up measurements, which gave a positive indication to proceed further with the survey. Existing drillings and test pit locations were not noticeable during geophysical surveying.

The survey consisted of 22 lines (L1–L22) in total. A line is one continuous entity of interrelated data points. A path is one line or a part of a line. Line L3 was measured back and forth across the landfill boundary, comprising a total of six short paths in a zig-zag formation (Figure 8). The same applies to Line 5, which consists of four separate paths. Altogether, 30 lines with paths either crossed the landfill boundaries or mapped the subsurface situation inside or outside the waste site. The intention was for each line or path to cross the estimated landfill boundary, with the exception of reference Lines L1 and L2.

Field notes, including a description of surface conditions and documentary photos, were taken after each measurement line. The dataset recorded consisted of 740 points. The shortest lines, L9 with 15 points and L18 and L22 with 18 points each, were approximately 30 m long. The longest line, L14 on the northern flank, had 77 points and a total length of 204 m, with an average interval between points of 2.7 m. Data from a line or path are presented as a symbol on the map, in profile form, or as a resistivity cross-section in this paper.

Data interpretation

The discussed reference Lines L1 and L2 provided a good basis for data interpretation. Indicators of anomalous landfill and waste disposal material are as follows:

- Strong point-to-point variability in Re-component and Im-component signal levels (gradient thousands per traverse metre).
- High values in Im-components and Re-components indicate low subsurface resistivities.
- A Re/Im ratio of >1 depicts good electrical conductors not found in normal ground. However, this only reliably applies when both Re and Im data give large values (thousands). In our case, the Re-component values are not absolute, but Re-component values and behaviour can be analysed and interpreted. Re/Im ratio is not presented in this connection but was calculated along with frequency-traverse apparent resistivities.
- Locations with negative minimum Re-component and Im-component values depict narrow conductors when they are situated between Tr-Rc coils. Negative Re-component values can also originate from material with high magnetic susceptibility.

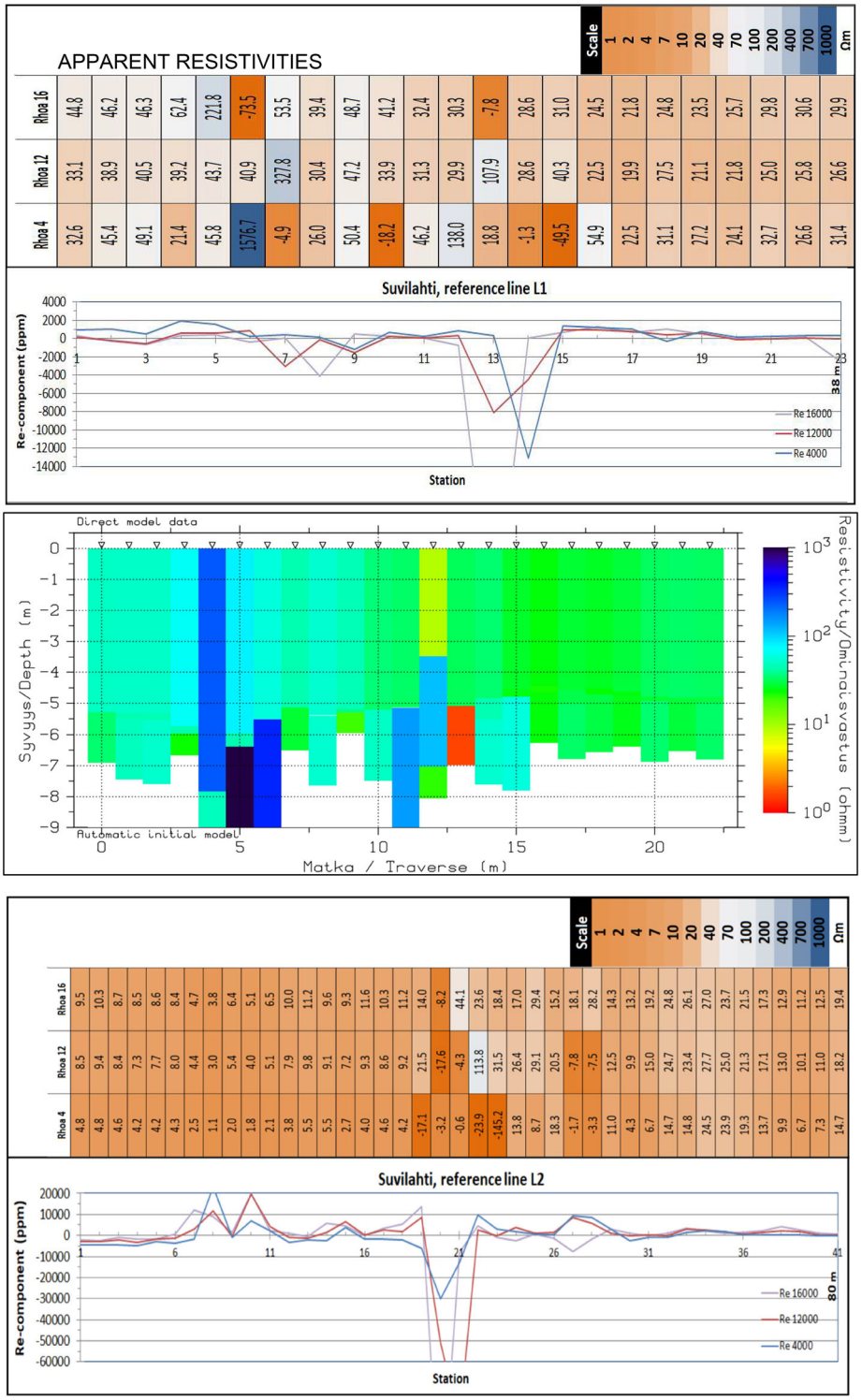

FIGURE 5 Natural soil and landfill area reference Line L1 and L2 results, resistivity frequency-traverse above, Re-component profile below. In the middle is the apparent resistivity pseudosection for Line L1. Rhoa + number (kHz) depict rows for respective apparent resistivity values at stations along lines L1 and L2.

- All resistivity values below 15–20 Ωm were considered potential waste fill, although in some lines, a return to a range over 20 Ωm was gradual.

We also applied a criterion that at least two EM frequencies need to indicate anomalous behaviour to filter out data recording errors from waste fill delineation. Each point showing any parameter value listed above was an anomaly indicating waste presence. Unavoidable surface objects influencing data were tracked in field notes, and respective points were removed from classified results.

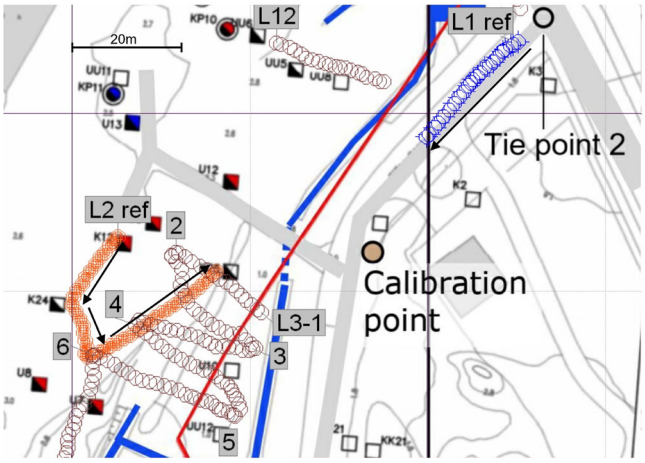

FIGURE 6 Reference line and station locations: Line L1, empty blue; Line L2, filled red circles), with investigation map on the background. The traverse direction is shown with arrows, and other content is as in Figure 1. The figure area frame is shown in Figure 3.

Points that contained waste material were sorted and marked on data profiles. Typically, there were no single-point anomalies. This is related to the fact that stations were spaced at intervals between 1.5 and 2.5 m, and the EMP-400 Profiler has, in a single 4-s recording, a footprint of several metres in all directions around the moving Tr-Rc middle point. Any object exceeding the detection limit influences two or more stations. On the other hand, separate waste objects and volumes can sum up in recorded responses.

A set of lines with representative results are shown. Frequently occurring typical responses and characteristics are illustrated by Figure 7. Line L4 (Figure 7 upper part) is an example of a continuous waste material response at stations 1–15 and natural ground at stations 16–20, with a total length of 35 m. The fill limit is detected at station 15. A waste response is demonstrated as very low resistivities of 2.2–16 Ωm, large negative Re-component values and an oscillating profile shape. In natural ground, all these features disappear instantly. Another typical feature for most lines was that in the waste deposit area, apparent resistivities are lower at lower frequencies, indicating EC that increases with depth. In natural ground, all frequencies yield high apparent resistivities, and the frequency effect is small or non-existent, indicating homogeneous layering.

Another type of response is observed along Line L6 in the eastern part of the study area (Figure 7 lower part). The profile starts from the waste fill area, and 3 separate major anomalies are situated at stations 3–6, 8–10 and 15–18. The line has a total length of 42 m. There is a very strong positive Re-component conductor anomaly at stations 2–3 and an anomaly showing strong negative Im-component values at station 16 with a varying Re-component. Exact landfill boundary delineation is difficult, but waste fill characteristics are missing after station 17, and at stations 20–21, apparent resistivities reach natural ground values (>20 Ωm). As previously, in waste fill, apparent resistivities decrease with depth, and in natural ground, the frequency effect is small.

RESULTS

Other profiles were interpreted in the same way that was described previously. All data points and classified results are presented in Figure 8. Red symbol denotes waste, empty circle no waste and grey gradual change between natural ground and waste. The measurement lines were placed quite well to cover the study area. The EM component data and resistivities calculated from all lines were interpreted and classified, supplemented with field notes and photos. The data are of high quality from an external noise perspective. The electrical power line, biogas line, surface objects and other cables did not significantly influence the data, or their influence at known locations was removed per point and from the final classified data.

Together with previous drill hole and test pit data, the landfill boundary was outlined more precisely. The new areas outside the pre-investigated landfill area are shown in Figure 8 as translucent orange areas. Areas inside the pre-investigation perimeter are shown in light blue. In many places, geophysics-based waste fill findings correspond well to the general outline estimated earlier. EM mapping findings indicate that waste fill sometimes forms long continuous passages, and in areas with less influenced ground, interlaced, scattered spots were discovered.

In the north, only small parts of geophysical profiles L12–L17 have clear anomalies indicating waste fill. In particular, Line L12 has only a few points indicating waste fill, although almost all nearby test pits contained waste. The eastern parts of L13 and L14 do not indicate waste fill either. In the south, the lines from L6 to L11 show that waste fill ends earlier in the south-east direction than indicated by the preceding investigation phase.

Data quality is an essential factor in the survey, and it influences the possibilities of data interpretation, such as the recognition of anomalies, and the reliability of the outcome. During a short survey like the Suvilahti case, data quality was controlled by multi-sample recordings at a calibration station and at a nearby resistive rock outcrop. The main statistical parameters from the calibration point (Figure 3) and from the outcrop reference point (outside the survey area) are shown in Table 1. The calibration point is located in a natural soil area in close proximity to the survey area. The results display consistent apparent resistivity of 30–31 Ωm at all frequencies. Standard deviations in the Im-component, which is particularly important, are small, between 14 and 34 ppm. The lowest frequency, 4 kHz, has the

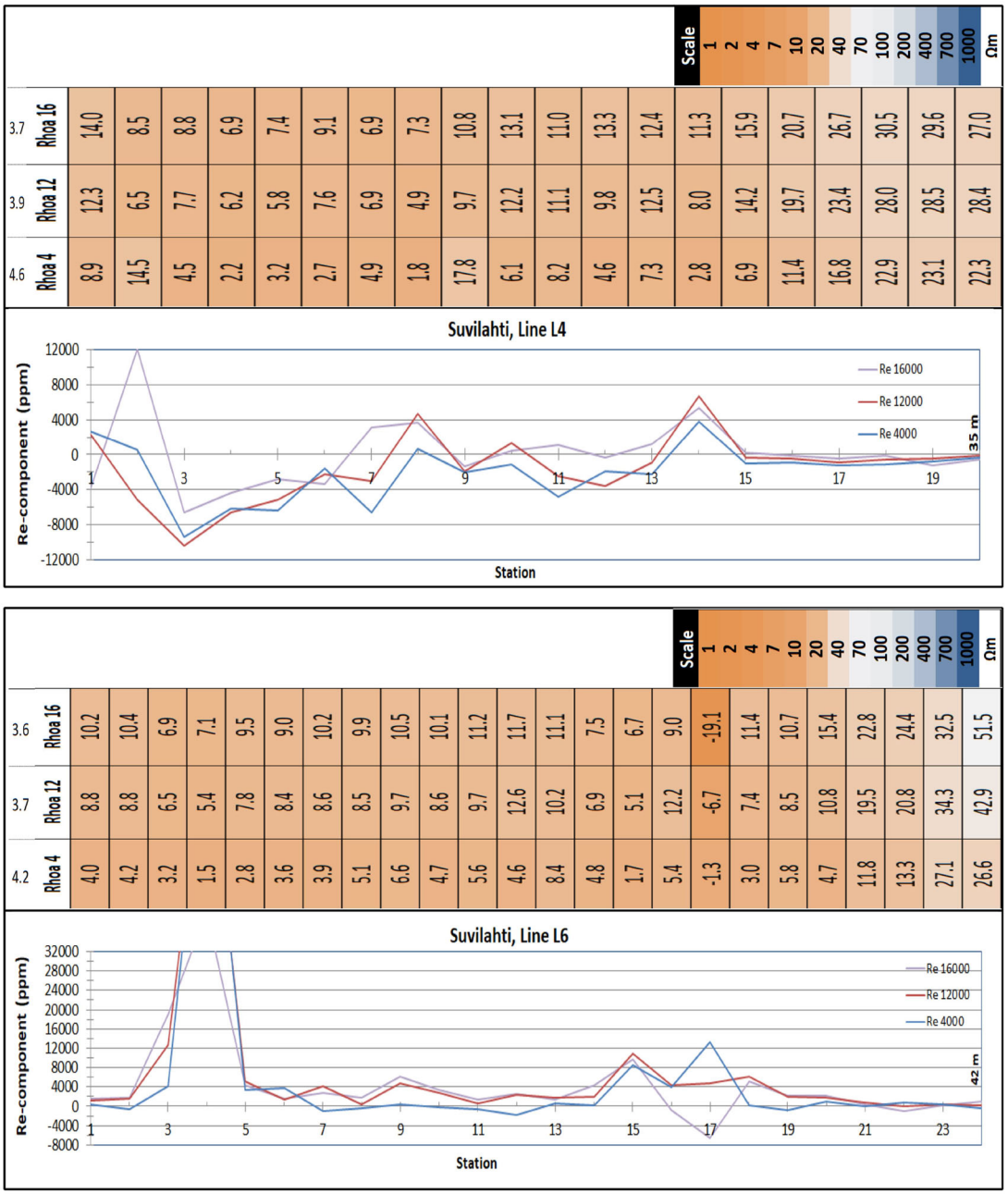

FIGURE 7 Line L4 (upper) showing continuous waste fill versus natural ground variation, Re-component profile and apparent resistivity pseudosection. Values left of the Rhoa-labels depict the average penetration depths at frequencies. Line L6 (lower) showing separate waste volumes and a gradual change from waste fill to natural ground, Re-component profile and apparent resistivity pseudosection.

highest standard deviation, both in ppm and percentage, and this is related to urban EM noise. The highest frequencies, 12 and 16 kHz, have very low standard deviations, less than 2% and 14–24 ppms. Re-components have higher standard deviations than Im-components, with the highest at a frequency of 4 kHz.

The bedrock outcrop location yielded very low Re-component and Im-component values, which was an expected and quality-assuring result. All frequencies showed apparent resistivities between 700 and 800 Ωm. Standard deviations are small, from 6 to 36 ppm, and in this case, the highest deviation was registered at a frequency of 16 kHz. At 12 kHz and 16 kHz frequencies, Re-component standard deviations were higher than at the on-site calibration point.

The outcrop point also provided data for static offset estimation. The offset values of 265, 165 and 10 ppm (4, 12 and 16 kHz, respectively) were calculated by setting resistive environment responses close to zero. These values were used for all data files as static offset

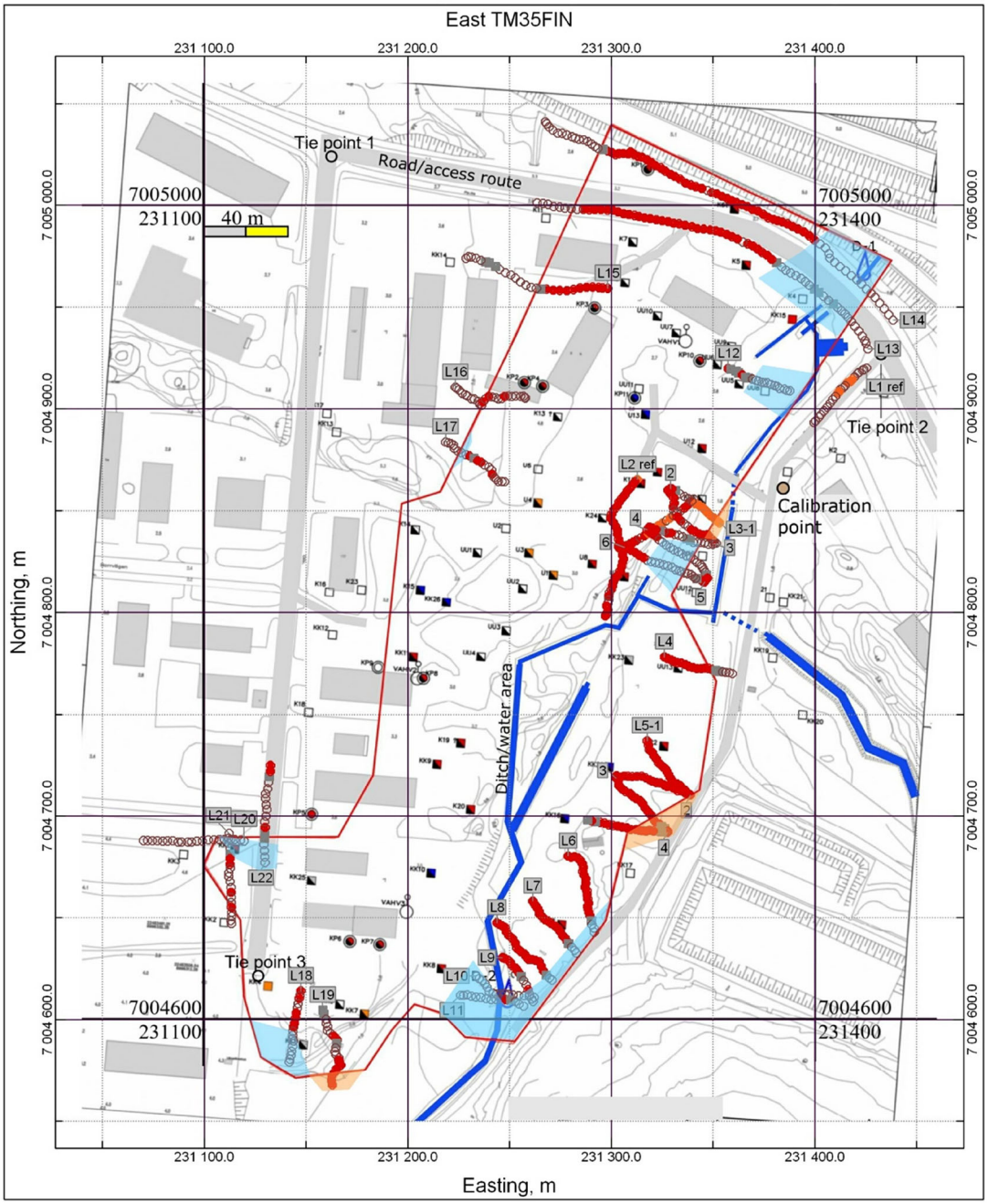

FIGURE 8 Classified EM data points indicating waste fill (red), natural ground characteristics (empty symbol) and transition points (grey). Supplementary landfill boundaries are indicated as light blue (no waste signature) and orange (waste) areas.

correction. Line profile data also showed that the determined static correction gave very consistent results, and in the resistive environment, values approached zero but did not yield negative values. Re-component levelling comes partly from the on-site calibration procedure and partly from the fine-tuning, when setting median values lower than the corresponding Im-component ones.

EM mapping results were compared at several points against drilling and test pit findings. There are 15 points where the distances between direct observations and EM profile data points are within 5 m. The nearest EM data point was compared with the direct observations. Hand-GPS positioning accuracy can cause a range of deviations of a few metres and influence the closest distance values. And it is to be noted that direct observation points were not marked at the site.

The comparison is presented in Table 2. Soil fill at observation points is divided into waste (grey fill) and no-waste categories. The degree of contamination is either

TABLE 1 Calibration and rock outcrop location data quality statistics.

Location	Parameter	Re 4000	Im 4000	Re 12,000	Im 12,000	Re 16,000	Im 16,000
Calibration point	Average (ppm)	87.0	354.4	142.1	1086.0	107.0	1450.4
8 recordings	Median (ppm)	84.0	359.5	137.0	1086.0	115.5	1454.0
Stacking 24	Standard deviation (ppm)	54.6	34.1	18.1	14.2	33.7	23.9
	Standard deviation (%)	62.7%	9.6%	12.7%	1.3%	31.5%	1.6%
	Apparent resistivity (Ωm)		30.7		30.5		30.4
	Induction number B		0.03		0.05		0.06
Bedrock outcrop	Average (ppm)	1.6	12.8	41.4	31.1	80.0	62.8
13 recordings	Median (ppm)	3.0	14.0	−11.0	35.0	24.0	60.0
Stacking 24	Standard deviation (ppm)	12.3	6.7	110.4	19.2	166.3	36.3
	Apparent resistivity (Ωm)		788		808		736
	Induction number B		0.01		0.01		0.01

at a hazardous waste level, exceeding the upper guideline value, or below the threshold value. For EM data, line, station and waste classification (cells with a grey background indicate waste) are given. Re/Im ratios and apparent resistivities are also given for frequencies of 4, 12 and 16 kHz at control points.

Table 2 shows that the geophysical classification correlates very well with direct observations. All waste-indicating EM data points are connected to waste-containing direct observations. There are five EM data points indicating no waste. Three of these have waste in direct observations; the concentration of hazardous substances is below the threshold value, at one point it exceeds the upper guideline value, and at another it exceeds the hazardous waste limit. Two direct observation points did not contain waste, and EM data points indicated the same result. There was waste in test pit KK1, and the concentrations of hazardous substances exceeded the hazardous waste value, but Point 4 on the nearest EM data Line L21 did not indicate a similar result at 2–3 m. This may describe the local heterogeneity of the waste fill, because neighbouring Points 5 and 6 along Line L21 did map the waste fill.

Table 2 also depicts the characteristic EM data values at the direct observation points. Mainly, low apparent resistivities detect waste fill objects. In some cases, a Re/Im ratio of >1 supports this well, but not always, as in Table 2, as shown by the three bottom rows and points KK5, KK1 and KK2. In addition, no waste-classified stations have apparent resistivities higher than the limit set, 20 Ωm. At one observation point, U7, apparent resistivities are >20 Ωm, but the Re/Im ratios of >1 and variation of values indicate waste fill influence. It can also be seen in Table 2 that when apparent resistivities reach a higher range, the Im-component and Re-component values are low, and the calculated ratios become more unstable with influencing noise.

It is an interesting question whether numerical modelling provides more in-depth results in a case like this, where high scattering, variability and heterogeneity of targeted objects are present. We did not apply 2D or 3D numerical modelling because the strongly varying total response consists of multiple small conductive objects. Instead, 1D layer modelling was tested for Line L13 to see how the waste fill volume in total differs from the surrounding natural ground.

Line L13 was selected for testing because it is long, completely crosses the presumed waste fill deposit, and runs along flat, homogeneous street pavement that contains no debris. Profile data are shown in the upper section of Figure 9, along with the frequency-traverse section showing the derived apparent resistivity. The lowest resistivity values are reached at traverses 80–82 m, at 100–103 m and at 148–151 m.

Depth penetration averages (all frequencies) for Line L13 are from 4.0 to 4.8 m following a rule and general modelling by Huang (2005) and Saksa (2016), implying the averaged $\sqrt{\delta}$ value (square root of skin depth). If the resistivity setting changes over the profile, depth penetration also varies, as will be observed in layer modelling. Depth penetration does not mean that all objects or layers within reach can be detected: Large objects and objects with high conductivity are easier to detect, resistive objects are not detected, and the target response must be considerably higher than noise in the recorded signal (see Table 1 and discussion of noise).

In modelling calculations, only Im-components were used (Re-component weights were set to zero). The programme EMDC1D was applied with a user-constrained starting model having three layers: a no-waste surface soil layer 1 m thick, a 2 m thick variable and potentially waste-containing layer and a thick bottom layer for underlaying natural soil. Bottom soil or clay is considered to form an electrically and effectively infinite layer. The surface layer resistivity was set to 200 Ωm, and the fix-free constraint was set to 1.0 (fixed = 1.0, 0.0 = free to change); the second layer was set to 30 Ωm, and the fix-free constraint was set to 0.0; and the bottom soil layer was set to 50 Ωm between clay or moraine at all points, and the fix-free constraint was set to 0.7, introduc-

TABLE 2 Comparison between observed waste classification from drillings and test pits versus classified electromagnetic (EM) data point results.

Observation drilling or pit		EMP measurement		Characteristic EM data values					
Code	Contamination	Line, station	Waste classification	Re/Im 4	Re/Im 12	Re/Im 16	Rhoa 4	Rhoa 12	Rhoa 16
K12	**Waste > dangerous limit**	L2 ref, 1	Yes	−1.9	−0.7	−0.5	4.8	8.5	9.5
K24	**Waste > dangerous limit**	L2 ref, 12	Yes	−1.1	−0.2	0.2	3.8	7.9	10.0
K25	Waste < below limits	L2 ref, 41	No	−0.1	0.2	0.3	14.7	18.2	19.4
K25	Waste < below limits	L3-1, 8	Yes	0.0	0.3	0.0	6.3	11.8	20.9
U7	**Waste > dangerous limit**	L3-6, 10	Yes	−0.5	1.6	1.9	22.8	−21.1	21.6
UU13	Waste < below limits	L4, 6	Yes	−0.4	−0.5	−0.7	2.7	7.6	9.1
K22	**Waste > dangerous limit**	L5-1, 4	Yes	−1.1	−0.2	0.1	3.0	6.8	7.7
KK18	**Waste > dangerous limit**	L7, 12	Yes	0.1	0.7	1.3	2.2	6.3	8.2
UU5	Waste < below limits	L12, 5	No	1.0	0.4	0.2	−104.1	48.7	28.5
UU8	No waste < below limits	L12, 14	No	−20.3	−1.6	−0.4	394.2	52.1	28.6
K67	**Waste > dangerous limit**	L14, 33	Yes	0.0	0.0	0.3	6.4	6.7	7.1
KP1	**Waste > dangerous limit**	L14, 50	Yes	1.0	1.3	1.3	2.0	4.9	6.5
KK5	Waste > overall limit	L18, 14	No	9.5	2.6	2.0	67.3	66.1	58.0
KK1	**Waste > dangerous limit**	L21, 4	No	−2.9	−0.4	0.4	33.8	41.5	47.0
KK2	No waste < below limits	L21, 20	No	−9.6	−3.7	−2.0	91.2	83.8	83.5
				Re/Im			**Rhoa**	**Ωm**	
				−5.0	0.0	5.0	**1**	**10**	**40**
							100	**400**	**1000**

ing higher stiffness in inversion but allowing changes. All layer thicknesses were fixed, so if layer thicknesses do vary, it is reflected in the layer resistivity values because conductance is the main electrical parameter determining each influencing conductive layer. Frequency normalization was set to inversion to counter the domination of high frequencies and their larger component values. Inversion cannot find proper solutions when Im-values are negative or at point-like anomalies when local minimum values appear above conductive 2D or 3D objects.

The inversion result for the three-layer model is given in the lower section of Figure 9. No data smoothing is applied (direct model data). Each optimization run consisted of 12 iterations, including a joint systematic and random search, and the global minimum found is the final model per station. The search window changes during the inversion process. In the example, a fitting improvement measured as a normalized RMS error was on average 4.6 times smaller in the final model than in the initial model.

Additional new information can be found in the outcome of the resistivity model. Low resistivities close to 1 Ωm occupy most of 65–155 m, where the average value for the middle layer is 3.4 Ωm. Resistivities <10 Ωm not typical to natural soil range from 54 to 65 m and from 157 to 170 m, possibly indicating gradual edges, but still the landfill area. The strongest responses are detected around 80, 100 and from 125 to 155 m. At the beginning of Line L13, natural soil seems to indicate typical clay values, but after 170 m, higher resistivities of ∼100 Ωm or higher may indicate moraine in addition to clay. It is also interesting to see the depth penetration curve behaviour. Throughout 60–160 m, depth penetration is 3–5 m, but at the end of the line, it reaches 7–8 m or even more. Depth penetration is plotted to result section as curve to show that layer information below the maximum depth is not covered by the EM survey. Modelling results with a depth penetration curve can show if the survey has covered the depth range of interest.

Some waste fill influence seems to creep to the bottom layer under the middle part of the profile. It is not

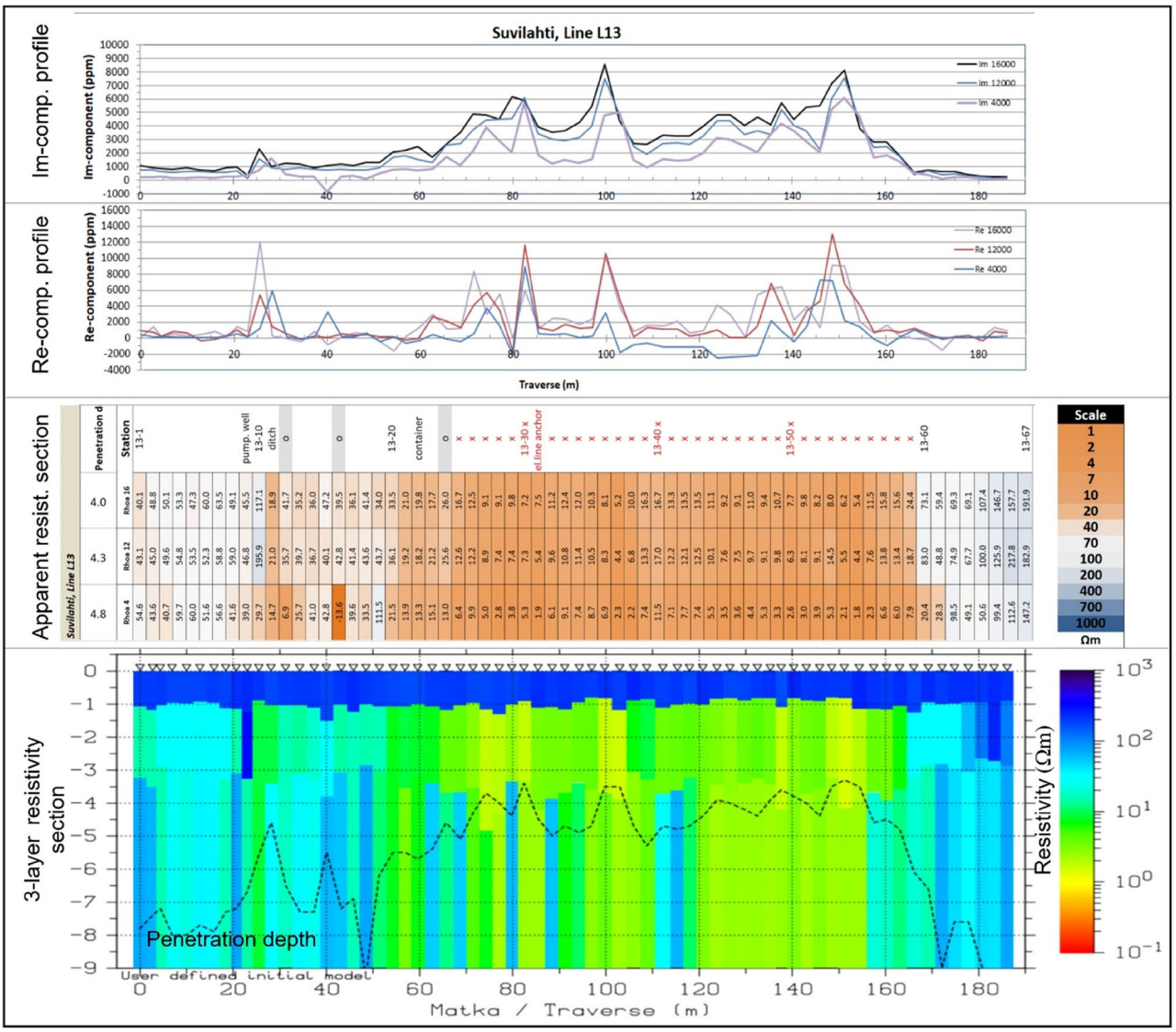

FIGURE 9 Line L13 profile data, apparent resistivity depth section and three-layer resistivity model. In modelling, major layer boundaries are set to 1 and 3 m, indicating the surface layer, potential waste fill layer with groundwater and bottom subsoil layer.

known on the basis of direct sampling if the waste has penetrated into the soil deeper than the typical 2-m-thick fill found.

Modelled waste volume resistivities are close to the low range of leachate water sample resistivities of 3–20 Ωm. Normally, layer resistivities are higher because of matrix influence and a low temperature close to +5°C in soil (water sample values are given at T = +25°C). It is probable that low values reflect the influence of the waste matrix and high EC of the leachate water together.

We conclude that in addition to frequency-traverse resistivity charts, 1D modelling can yield supplementary results from subsurface structure and resistivity. It also uses EM component values and physical depth penetration coverage reliably and follows underlying EM theory.

A further post-modelling study was carried out to study magnetic susceptibility changes along the profile. Magnetic susceptibility variation only influences Re-component values, and therefore, Re-components contain influences both from EC and magnetic susceptibility. Research by Won and Huang (2004) indicated that with short-coil spacing systems, a magnetized layer at depths of tens of centimetres or more causes a negative Re-component response. Having a 1 m non-magnetic surface layer means that magnetic susceptibility causes negative Re-component anomalies. Their calculation scheme also involves limits on applicable frequency and EC of the host mass. Regarding Line L13, this means that magnetic susceptibility is mainly visible at a low frequency of 4 kHz and that low resistivity below 10 Ωm does not allow accurate calculation.

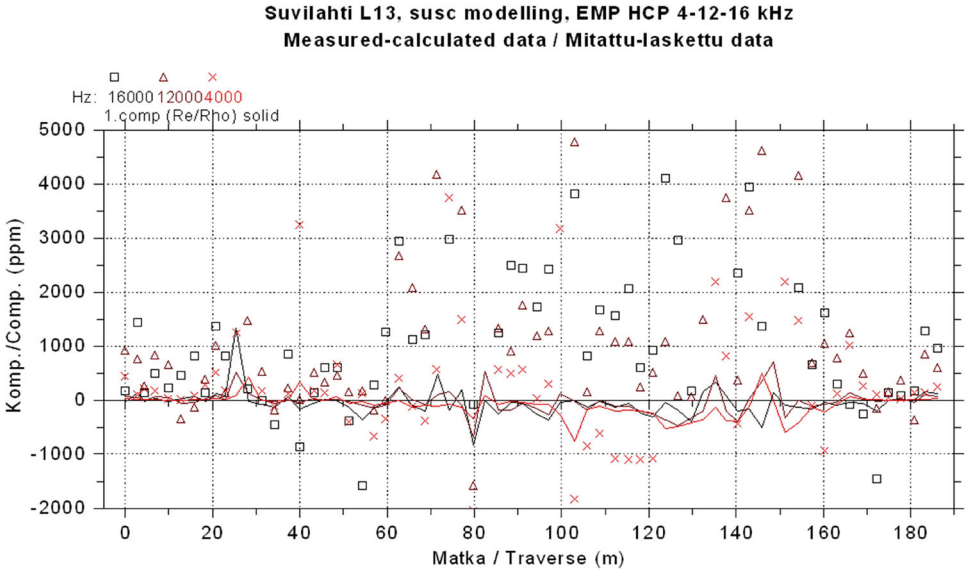

FIGURE 10 Scattering of Re-component values (points) and deduced Re-component profiles after magnetic susceptibility modelling (solid lines).

Despite these limits, the EMCONVERTER software module was used to calculate the magnetic susceptibility of the bottom layer (below 1 m). The process consists of three steps: (a) Re-component scaling based on Im-component values, (b) subtraction of the EC response from the Re-component values and (c) calculating magnetic susceptibilities using Re-component data residuals for the layer modelled.

At each point, the dataset is processed, and the estimated magnetic susceptibility is the average for applicable frequencies at that point. All points that do not exhibit magnetic susceptibility or have low resistivity remain non-determined. As pointed out earlier, calculations found no valid points for magnetic susceptibility conversion. However, processed Re-component line data indicate some areas where the effects of magnetic susceptibility are still clear (Figure 10). It is evident that between 55 and 160 m, traverse, almost continuously negative Re-components at several frequencies indicate the presence of magnetic materials. Findings support the interpretation of waste fill and determined waste distribution based on resistivities.

DISCUSSION

Ground electrical resistivity has been an important factor in assessing the boundaries of the waste disposal area, as shown in the profile data examples. In natural conditions, soil types and water EC govern the values obtained. Two additional factors that were considered and which may potentially influence the outcome are brackish sea water and the presence of acid sulphate soils.

The investigation site lies at a low topographical (1–4 m) level and borders the sea shore to the south. Brackish sea water near the surface has an EC of 720–1000 mS/m (1.0–1.4 Ωm) and may have temporarily flooded to the site area during periods of high sea levels. Between 1991 and 2020, the highest maximum at Vaasa was +153 cm, and the average maximum is +104 cm (Finnish Meteorological Institute, 2022).

Most of the area is situated between elevations of +2…+4 m, and sea water does not flood the area. Only the southernmost corner where Lines L8–L11 and L19 are situated may have been influenced by salt from sea water. Lines L8 and L9 in the south were compared against Line L4 further to the north, and resistivities at the presumed landfill area and natural ground are very similar. The waste disposal area does not form a topographical depression, and the presumed landfill boundaries do not correlate with any topography variations. It is concluded that brackish water intrusion has no influence upon the site's resistivity structure and waste delineation.

Acid sulphate soils are frequently found in the Vaasa region. Most drilled points around the Suvilahti area of Vaasa have an acid sulphate layer starting at a depth of 1.0–2.0 m (Geological Survey of Finland, 2022). The presence of acid sulphate soils was not studied at Suvilahti in penetrative and sample-based studies. In non-disturbed conditions, the layer is situated below the groundwater surface, but a lowering of groundwater may induce acidic runoff, leaching metals from the soil. If soil acidification takes place, the amount of dissolved substances increases, and water may even reach high EC values, up to 1400–2000 mS/m.

In the case of Suvilahti, it is likely that acid sulphide clays are present. A waste layer of 0.5–2.0 m in thickness may have reached the sulphate clay. Groundwater and the surface water level are close to the ground surface and above the sulphate clay layer. In addition, representative water samples do not display high EC values, quantities of dissolved metals are moderate, and pH levels remain within the 6.6–7.4 neutral range (Vahanen Environment, 2015). Therefore, we estimate that acid sulphate clays and soil acidification have not influenced geophysical and resistivity-based waste deposit delineation.

CONCLUSIONS

EM results (in Figure 8) pointed out new landfill boundary positions, confirmed in places the previous ones and showed some areas that did not have any waste material indications at all. The classified points also indicate the type of waste fill, either as scattered waste fill or more continuous fill along each line. In conclusion, the geophysical EM mapping approach was efficient with the use of reference and investigation lines. It can be and was challenging to find good reference lines both for representative natural soil and waste conditions. The approach of making individual lines at applicable locations was a sound method; a systematic line network for mapping would not have been feasible because of the access-limiting obstacles and the large amount of work required to cover the whole area.

From a quality perspective, it is also favourable to make reference lines first. In natural ground conditions, smooth signal characteristics indicate that the instrument works properly, and EM noise conditions in the urban area do not jeopardize surveying. EM measurement was likely the most efficient method to delineate waste deposits in the given site conditions. The timing after drillings and test pits was also correct, and site data enabled the optimization of rapid geophysical mapping and aided in interpretation.

The developed EM data classification method worked reliably, and results were consistent with direct sampling reference data. Developed and used frequency-traverse apparent resistivity section presentation fits well to EM data characteristics, presents multi-frequency data in a useful graphical layout and does not contain non-necessary averaging or inherent side effects of depth coverage variation.

In this case, numerical modelling only provides a limited amount of added value for anomaly detection. Modelling can provide some insight into resistivity and volumetrics, for example, by allowing the assessment of ground and waste matrix type, variations within a specific ground layer or estimates for the ionic strength of water.

Finally, it was interesting to find a clear and discrete waste deposit boundary against natural soils in most places, even after a long period had passed since waste disposal activity. It may be that clay formation, due to its very low hydraulic conductivity, has kept leachate inside the waste deposit volume. If so, this would explain why water with a high ionic strength and high EC has stayed in the waste deposit and retained a distinct boundary with natural surroundings.

ACKNOWLEDGEMENTS

We would like to thank the City of Vaasa and the real estate sector manager Christoffer Rönnlund for permission to publish the data from the Suvilahti site investigations and the geophysical electromagnetic surveying results. We would like to thank Stacy Blyth at Verbum Kielipalvelut for revising the English of the manuscript.

DATA AVAILABILITY STATEMENT

The field data that support the findings of this study are not available. The theoretical calculation data (Figure 2) are available from the corresponding author.

REFERENCES

Andrade, F.C.M., Fischer, T. & Valenta, J. (2016) Study of errors in conductivity meters using the low induction number approximation and how to overcome them. *EAGE near surface geophysics, conference 2016*. Extended abstract we 22P2 24. Utrecht, the Netherlands, European Association of Geoscientists & Engineers. p. 5.

Delgado-Rodriguez, O. (2017) Mapping of hydrocarbon- and scrap-metal-contaminated soil using volatile organic compounds and electromagnetic profiling methods. *Near Surface Geophysics*, 15, 312–321.

Dumont, G., Robert, T., Marck, N. & Nguyen, F. (2017) Assessment of multiple geophysical techniques for the characterization of municipal waste deposit sites. *Journal of Applied Geophysics*, 145, 74–83.

Finnish Meteorological Institute. (2022) Available from: https://en.ilmatieteenlaitos.fi/sealevelstatistics.html

Frischknecht, F.C., Labson, V.F., Spies, B.R. & Anderson, W.L. (1991) Profiling methods using small sources. In: Nabighian, M.N. (Ed.) *Electromagnetic methods in applied geophysics*. Houston, TX: Society of Exploration Geophysicists, pp. 105–270.

Geological Survey of Finland. (2022) *Acid sulphate soils map service (in Finnish)*. Available at: https://gtkdata.gtk.fi/hasu/index.html

Godio, A. & Naldi, M. (2009) Integration of electrical and electromagnetic investigation for contaminated site. *American Journal of Environmental Sciences*, 5(4), 561–568.

Huang, H. (2005) Depth of investigation for small broadband electromagnetic sensors. *Geophysics*, 70(6), G135–G142.

Inauen, C.M., Chambers, J.E., Watlet, A., Whiteley, J.S., Gunn, D.A., Dashwood, B. et al. (2019) Landfill characterization with a multi-method geophysical approach—a case study from Emersons Green, UK. *Proceedings of near surface geoscience conference, 2019*. Extended abstract we_25_P15. The Hague, Netherlands, European Association of Geoscientists & Engineers. pp. 1–5.

McNeill, J.D. (1980) *Electromagnetic terrain conductivity measurement at low induction numbers*. Canada: Geonics Limited.

Mitsuhata, Y., Ando, D., Imasato, T. & Tahagi, K. (2014) Characterisation of organic-contaminated ground by a combination of electromagnetic mapping and direct-push in situ measurements. *Near Surface Geophysics*, 12, 613–621.

Mitsuhata, Y., Ueda, T., Kamimura, A., Kato, S., Takeuchi, A., Aduma, C. & Yokota, T. (2022) Development of a drone-borne electromagnetic survey system for searching for buried vehicles and soil resistivity mapping. *Near Surface Geophysics*, 20, 16–29.

Narciso, J., Azevedo, L., Van De Vijver, E. & Van Meirvenne, M. (2020) Geostatistical electromagnetic inversion for landfill characterisation [Expanded abstracts]. *Near Surface Geoscience Conference & Exhibition Online 2020*, European Association of Geoscientists & Engineers. pp. 1–5.

Reynolds, J.M. (2011) *An introduction to applied and environmental geophysics*, 2nd edition, Hoboken, NJ: Wiley-Blackwell.

Saksa, P. (2016) Frequency effects in hand-held electromagnetic short coil spacing data. Proceeding of poster presentation, *EAGE annual conference, WIEN 2016*. Utrecht, the Netherlands, European Association of Geoscientists & Engineers. pp. 1–5.

Soveri, J., Mäkinen, R. & Peltonen, K. (2001) *Pohjaveden korkeuden ja laadun vaihteluista Suomessa 1975–1999*. Suomen ympäristö 420. Suomen ympäristökeskus Helsinki (in Finnish).

Spies, B.R. & Frischknecht, F.C. (1991) Electromagnetic sounding. In: Nabighian, M.N. (Ed.) *Electromagnetic methods in applied geophysics*. Houston, TX: Society of Exploration Geophysicists, pp. 285–426.

Vahanen Environment Oy. (2015) *Environmental investigation report; Suvilahti, old landfill area*. Vahanen Environment Oy. Report ENV605.

Won, I.J. (2003) Small frequency-domain electromagnetic induction sensors. *The Leading Edge*, 22, 320–322.

Won, I.J. & Huang, H. (2004) Magnetometers and electro-magnetomenters. *The Leading Edge*, 23, 448–451.

How to cite this article: Saksa, P. & Vepsäläinen, M. (2025) Electromagnetic survey of old landfill boundaries—A case study. *Near Surface Geophysics*, 23, 153–172. https://doi.org/10.1002/nsg.70004